

Hidden Genes Genetic Algorithm for Multi-Gravity-Assist Trajectories Optimization

Ahmed Gad* and Ossama Abdelkhalik†

Michigan Technological University, Houghton, Michigan 49931-1295.

DOI: 10.2514/1.52642

The problem of optimal design of a multi-gravity-assist space trajectory, with a free number of deep space maneuvers, poses a multimodal cost function. In the general form of the problem, the number of design variables is solution dependent. This paper presents a genetic-based method developed to handle global optimization problems where the number of design variables vary from one solution to another. A fixed length for the design variables is assigned for all solutions. Independent variables of each solution are divided into effective and ineffective segments. Ineffective segments (hidden genes) are excluded in cost function evaluations. Full-length solutions undergo standard genetic operations. This new method is applied to several interplanetary trajectory design problems. This method has the capability to determine the number of swing-bys, the planets to swing by, launch and arrival dates, and the number of deep space maneuvers, as well as their locations, magnitudes, and directions, in an optimal sense. The results presented in this paper show that solutions obtained using this tool match known solutions for complex case studies.

Nomenclature

A	=	continuous design variable
B	=	discrete design variable
C	=	transformation matrix
F	=	fitness (cost function)
f	=	flight direction
h	=	pericenter altitude, km
\bar{h}	=	normalized swing-by pericenter altitude
i	=	maximum possible number of swing-by maneuvers
j	=	maximum possible number of total deep space maneuvers in whole trajectory
k	=	maximum number of independent thrust impulses
l	=	leg number
L_{\max}	=	maximum chromosome length
m	=	number of swing-by maneuvers
n	=	number of deep space maneuvers in single leg
P	=	planet identification number
q	=	number of bits
R	=	mean radius, km
\mathbf{r}	=	heliocentric position vector in inertial frame, km
r_{per}	=	pericenter radius, km
\mathbf{r}_{per}	=	pericenter radius vector, km
T	=	time of flight, days
t	=	Julian date
\mathbf{v}	=	heliocentric velocity vector in inertial frame, km/s
\mathbf{v}_{∞}	=	hyperbolic velocity vector relative to planet, km/s
v_{∞}	=	hyperbolic speed relative to planet, km/s
z	=	number of swing-bys followed by zero-deep-space-maneuver trajectory
Γ	=	intersection line between Π and inertial ecliptic plane
Δ	=	accuracy of continuous design variable
δ	=	deflection angle in swing-by plane, rad

$\Delta \mathbf{v}$	=	impulsive maneuver velocity vector, km/s
Δv_T	=	total mission cost, km/s
ε	=	epoch of deep space maneuver as a fraction of transfer time
η	=	swing-by plane rotation angle, rad
ι	=	inclination of Π to ecliptic, rad
μ	=	gravitational constant, km ³ /s ²
Π	=	perpendicular plane to incoming relative velocity
Ω	=	angle between Γ and inertial \hat{I} , rad

Subscripts

a	=	arrival
d	=	departure
L	=	local frame
l	=	leg
max	=	maximum
min	=	minimum
nps	=	nonpowered swing-by
p	=	swing-by planet
ps	=	powered swing-by
req	=	required
s/c	=	spacecraft

Superscripts

–	=	incoming
+	=	outgoing

I. Introduction

THE optimization of interplanetary trajectories continues to generate a great deal of interest [1,2]. In interplanetary missions, it is usually desired to send a spacecraft to rendezvous with a planet or an asteroid. The interplanetary trajectory design problem can be addressed in either a two-body or a three-body dynamics framework. It can be addressed assuming impulsive or continuous thrust. The patched conic approach for interplanetary trajectory design assumes a two-body dynamics model and the use of chemical propulsion system only [3]. In patched conic mission design, it is observed that a deep space maneuver (DSM) may reduce the cost of a simple two-impulse interplanetary transfer [e.g., the cost of the Earth–Mars (EM) mission can be reduced by adding an impulse, almost midway, in addition to the initial and final impulses]. For a transfer between two noncoplanar orbits, a DSM reduces the out-of-plane component of

Received 4 October 2010; revision received 11 January 2011; accepted for publication 12 January 2011. Copyright © 2011 by the American Institute of Aeronautics and Astronautics, Inc. All rights reserved. Copies of this paper may be made for personal or internal use, on condition that the copier pay the \$10.00 per-copy fee to the Copyright Clearance Center, Inc., 222 Rosewood Drive, Danvers, MA 01923; include the code 0022-4650/11 and \$10.00 in correspondence with the CCC.

*Ph.D. Candidate, Mechanical Engineering–Engineering Mechanics Department, 815 R. L. Smith Building, 1400 Townsend Drive; ahgadels@mtu.edu.

†Assistant Professor, Mechanical Engineering–Engineering Mechanics Department, 815 R. L. Smith Building, 1400 Townsend Drive; oabdelk@mtu.edu. Member AIAA.

the required impulsive velocity, and thus the total mission cost Δv_T [4]. Because of Δv leveraging effect at large distances from the sun, DSMs are used to reduce the required Δv_T , and hence the equivalent propellant mass that allows for a larger size payload or a smaller launch vehicle. Navagh applied the primer vector theory to determine where and when to use a single DSM to reduce the cost of a trajectory [4]. He applied DSMs to a Mars round-trip mission to determine their effect on the launch opportunities. He also studied cycler trajectories and Mars mission abort scenarios. Later, Abilleira investigated the broken-plane maneuver impact on the total mission cost Δv_T , the incoming relative velocity, and the launch energy for Earth-to-Mars trajectories [5]. He suggested the extra Δv be applied close to the halfway point of the near-180 deg transfer. He mentioned that DSMs could also allow new families of trajectories that would satisfy very specific mission requirements not achievable with ballistic trajectories [5].

The optimization problem, in its general form, aims to minimize some cost functions: usually the overall cost of the mission in terms of the fuel expenditure. Another possibility is to optimize the mission trajectory to achieve minimum mission duration. Interplanetary missions usually employ gravity-assist maneuvers to reduce the overall cost of the mission. The launch and arrival dates also affect the mission cost. The space trajectory optimization process must therefore determine the optimal values for the following parameters: the departure and arrival dates, the number of swing-bys, the planets to swing by, and the number of DSMs and their magnitudes, directions, and locations. This optimization problem, in its general form, is challenging. Several optimization algorithms were developed in the literature. Izzo et al. developed a deterministic search space pruning algorithm to investigate the problem of multiple-gravity-assist (MGA) interplanetary trajectories design [6]. The developed tool requires the user to specify the gravity-assist sequence (i.e., the number of swing-bys and the planets to swing by), and the pruning technique efficiently locates all the interesting parts in the search space of the DSM variables [6]. Olympio and Marmorat [7] studied the global optimization of MGA trajectories with DSMs (MGADSMs). They implemented a pruning strategy on the search space to find fit trajectories. To that end, a stochastic initialization procedure, combined with a local optimization tool, was used to provide a set of locally optimal solutions. The primer vector theory was extended to study the MGA trajectories. The optimal number of DSMs was determined as well as their magnitudes and directions. This technique was verified using several interplanetary mission case studies. An efficient local optimization algorithm was applied to find a solution for complex problems [7]. In this method, the user specifies the sequence of swing-bys a priori. Later, Olympio and Izzo applied the interaction prediction principle to decompose the MGA problem into subproblems by introducing and relaxing boundary conditions [8]. Parallel subproblems could then be solved. The algorithm was able to efficiently calculate the optimum number of DSM impulses and their locations.

Evolutionary algorithms were implemented to solve the MGADSM problem [9,10]. Vasile and Pascale used an evolutionary algorithm with a systematic branching strategy to optimize the problem of MGADSM [9]. They developed a design tool (IMAGO) that allowed for more exploration of the solution domain through balancing the local convergence and the global search. The search space was reduced by performing a deterministic step at every new run. The tool was applied several times on each specific problem to provide reliable results [9]. IMAGO was able to calculate many typical optimal sequences for a Jupiter mission. For the complex trajectories (Cassini and Rosetta missions [11]), IMAGO was used assuming a fixed planet sequence and wide ranges of design variables based on a priori knowledge of the solution space [9]. Olds et al. developed a trajectory optimization tool (MDTOP) to perform preliminary design of high-thrust interplanetary missions using the differential evolution (DE) strategy [10]. They tuned the algorithm parameters to improve DE performance and were able to solve complex interplanetary missions, such as Cassini and Galileo [10,11]. A formulation for the N -impulse orbit transfer that integrates evolutionary algorithms and a Lambert's problem formalism results

in a more efficient search algorithm [9,12]. This integration of Lambert's problem significantly reduces the size of the design space to include only candidate solutions that satisfy Lambert's problem solution. In that context, the genetic algorithm (GA) was implemented to obtain the optimum impulses for noncoplanar elliptical interplanetary orbit transfers [12,13].

GAs have been widely used in the literature to solve several orbital mechanics problems. GAs have been used to solve the fuel-optimal spacecraft rendezvous problem [14], to design orbits with lower average revisit times over a particular target site [15], to design natural orbits for ground surveillance [16], to design constellations for zonal coverage [17], and to investigate the design of near-optimal low-thrust orbit transfers [18]. GAs are optimization techniques, based on the Darwinian principle of the survival of the fittest, that perform a stochastic search of initial conditions that maximize a given fitness function [19]. The GAs have global search capability, and they do not require derivatives [17]. GAs are particularly efficient for the type of problems where it is not necessary to find the optimal solution but, rather, a few reasonably good solutions. In GA, a design point is called a chromosome (string). Each string consists of a set of independent design variables that define a candidate solution to the problem. Chromosomes are composed of genes (features) that take on different alleles (values) [19]. Associated with each gene is its location in the chromosome. The initial population consists of a finite number of randomly generated individuals. Generations of this population are created using genetic operations such as selection, crossover, and mutation. At each generation, the fittest individuals are selected as a pool of parents. The fitness of each individual is evaluated according to the cost function. These parents are then used to create the new generation. This process leads to the evolution of more fit populations. Dasgupta and McGregor developed a structured GA [20]. They introduced the terms of active and passive genes through applying a gene activation mechanism that uses a multilayered structure for the chromosome. Kim and de Weck proposed a variable chromosome length genetic algorithm (VCL-GA) in structural applications [21]. The variable chromosome length concept depends on gradually increasing the chromosome length in subsequent stages to achieve progressive refinement. Increasing the chromosome length was proposed by either adding new design variables or refining the current ones [21].

As can be seen from the previous discussion, often the mission designer determines the number of swing-bys and selects the planets to swing by by hand. The motivation of this study is to develop an optimization algorithm that can, without a priori knowledge, compute the number of swing-bys and the planets to swing by, in addition to the rest of the classical MGADSM design variables. This is a complex problem characterized by the following: first, some of the design variables are discrete; second, the number of design variables is solution dependent; and finally, the number of design variables becomes rather high in complex missions. There are many types of evolutionary algorithms, such as particle swarm [22] and DE [9,10], which have been used to solve trajectory optimization problems. But neither of those methods handles discrete design variables (DDVs). The fact that some of the design variables are discrete suggests the use of GAs [23,24]. Solution-dependent design variables mean that different solutions have different numbers of design variables. This fact hinders the implementation of standard GAs in optimization. In this paper, the concept of hidden genes is introduced in GA optimization. This concept allows the handling of all solutions in the design space as if they all have the same string length, and hence enables the implementation of standard genetic operations. This paper presents an optimization algorithm and a software tool that have the capabilities to find, in an optimal sense, the values for the following design variables: optimal number of swing-bys, the planets to swing by, the times of swing-bys, the optimal number of DSMs, the components of these DSMs, the times at which these DSMs are applied, the optimal launch and arrival dates, and the optimal flight direction for the mission. The search space of the new algorithm includes solutions with multirevolution trajectories. The software tool for interplanetary trajectory optimization using hidden genes genetic algorithm (ITO-HGGA) is

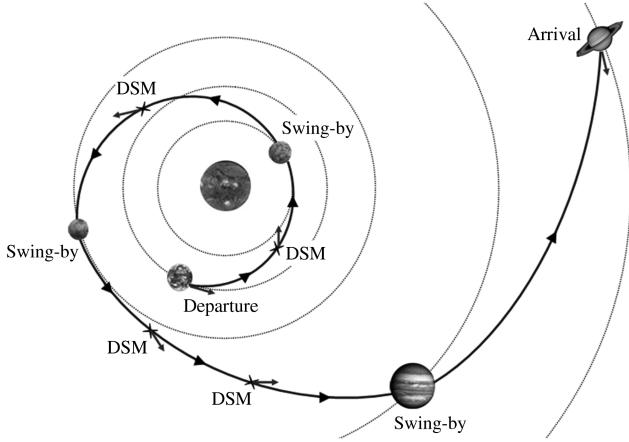


Fig. 1 MGA trajectory with free number of DSMs (MGADSMs).

developed. ITO-HGGA is tested for a number of MGADSM design problems and compared with known solutions in the literature.

II. Problem Formulation

The objective is to design an interplanetary trajectory for a spacecraft to travel from the departure planet to the target planet with a minimum cost. The spacecraft will benefit from as many swing-bys as needed of other planets. The spacecraft can also apply DSMs. The segment between any two planets is called a leg. A leg can have any number of DSMs, as seen in Fig. 1. The spacecraft may have multiple revolutions about the sun before proceeding to the next planet. The scenario of the mission refers to the sequence of swing-bys. The determination of the mission scenario then means the determination of the number of swing-bys, the planets of swing-bys, and the times of swing-bys. The problem is worked out in a two-body dynamics framework, and it is formulated as an optimization problem.

The problem is formulated as follows. For given ranges for departure and arrival dates from the departure planet to a target planet, find the optimal selections for the number of swing-bys, the planets to swing by, the times of swing-bys, the number of DSMs, the components and directions of these DSMs, the times at which these DSMs are applied, and the exact launch and arrival dates such that the total mission cost Δv_T is minimized.

III. Dependent Variables

An essential step in any genetic optimization algorithm is to evaluate the cost function at different design points. At each design point, the optimization algorithm selects values for all the independent design variables of the problem. There are several other dependent variables that need to be computed before the cost function can be evaluated. This section details how these dependent variables are computed given a set of values for the independent design variables.

A. N -Impulses Trajectory

In the simple case of a two-impulse interplanetary orbit transfer, the total number of design variables is two [13]. In this case, the trajectory has one leg between the departure and arrival planets. The two variables are the departure and arrival dates. For a candidate solution, the departure and arrival dates fix the time of flight (TOF) T . A Lambert's problem is then solved to find the transfer orbit. The required departure and arrival impulses, $\Delta \mathbf{v}_d$ and $\Delta \mathbf{v}_a$, are then calculated.

In an N -impulses trajectory (no swing-bys), there are n DSMs in addition to the departure and arrival impulses. The number of different orbits is $n + 1$. The number of unknowns in this case is $4(n + 2)$. These unknowns are the impulse velocity increment vectors $\Delta \mathbf{v}$ and the times of applying them t for all impulses. The time of application of each DSM is defined as a fraction ε of the overall

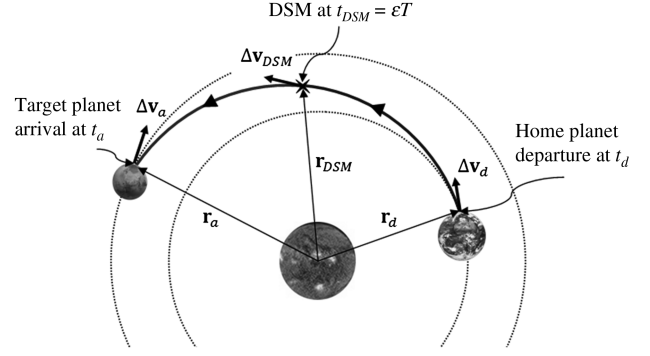


Fig. 2 Three-impulse transfer orbit.

transfer time T . So, $t_{DSM} = \varepsilon T$, where $0 < \varepsilon < 1$. Figure 2 shows a three-impulse trajectory (one DSM).

Of the $4(n + 2)$ unknowns, there are $4n + 2$ independent design variables. These independent variables are selected to be the departure and arrival dates, the velocity increment vector(s) at the first n impulses, and the fractional variable(s) ε at each DSM. The remaining six unknowns are computed as functions of the independent design variables as follows: the departure and arrival dates fix the departure and target planets positions; hence, the spacecraft heliocentric positions at these two locations, \mathbf{r}_d and \mathbf{r}_a , are fixed. The impulsive velocity vector at departure $\Delta \mathbf{v}_d$ yields the spacecraft initial velocity on the first transfer orbit that, along with \mathbf{r}_d , fixes the first transfer orbit. Once we have the first transfer orbit and are using the time of applying the first DSM ε_1 , the location of the first DSM is computed using Kepler's equation [25]. The velocity of the spacecraft at that location before applying the DSM is also computed. The velocity increment at the first DSM is used to compute the spacecraft velocity right after the first DSM is applied. The procedure used in the first transfer orbit is repeated for all subsequent transfer orbits but the last one. On the last transfer orbit, Lambert's problem is solved. The spacecraft positions at the last DSM and at arrival are known. The TOF is also known. A Lambert solution yields the last transfer orbit. The velocity increments at the last DSM and at arrival are then computed. The total cost of the mission in this case is

$$\Delta v_T = \|\Delta \mathbf{v}_d\| + \sum_{i=1}^n \|\Delta \mathbf{v}_{DSM_i}\| + \|\Delta \mathbf{v}_a\| \quad (1)$$

B. Gravity-Assist Maneuvers

In this analysis, a gravity-assist maneuver is assumed to be an instantaneous impulse applied to the spacecraft. The spacecraft heliocentric position vector is assumed not to change during the swing-by maneuver, and it is equal to the swing-by planet heliocentric position vector at the swing-by instance:

$$\mathbf{r}^- = \mathbf{r}^+ = \mathbf{r}_p \quad (2)$$

where \mathbf{r}^- and \mathbf{r}^+ are the spacecraft incoming and outgoing heliocentric position vectors, respectively, and \mathbf{r}_p is the swing-by planet heliocentric position vector.

As shown in Fig. 3, the trajectory of the spacecraft relative to the planet is a hyperbola with the relative hyperbolic velocity vector \mathbf{v}_∞ , which is defined as [26]

$$\mathbf{v}_\infty = \mathbf{v}_{s/c} - \mathbf{v}_p \quad (3)$$

where $\mathbf{v}_{s/c}$ and \mathbf{v}_p are the spacecraft and planet heliocentric velocity vectors at the swing-by instance, respectively.

Two types of swing-bys are implemented in this work: powered swing-bys and nonpowered swing-bys [7]. In a nonpowered swing-by, the incoming and outgoing relative velocities, \mathbf{v}_∞^- and \mathbf{v}_∞^+ , respectively, have the same magnitude:

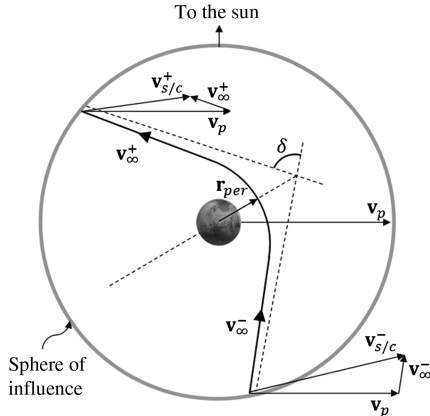


Fig. 3 Gravity-assist model as seen in the swing-by plane projection.

$$\|\mathbf{v}_{\infty}^{-}\| = \|\mathbf{v}_{\infty}^{+}\| = v_{\infty} \quad (4)$$

The swing-by plane is defined by the incoming relative velocity vector \mathbf{v}_{∞}^{-} and the pericenter radius vector \mathbf{r}_{per} . The change in the relative velocity direction in the swing-by plane δ can be computed from Eq. (5) [26]:

$$\sin(\delta/2) = \frac{\mu_p}{\mu_p + r_{\text{per}} v_{\infty}^2} \quad (5)$$

where μ_p is the gravitational constant of the swing-by planet, and $r_{\text{per}} = \|\mathbf{r}_{\text{per}}\|$. In a nonpowered swing-by, the spacecraft velocity change is given by Eq. (6) [7]:

$$\|\Delta \mathbf{v}_{\text{nps}}\| = \|\mathbf{v}_{\infty}^{+} - \mathbf{v}_{\infty}^{-}\| = 2v_{\infty} \sin(\delta/2) \quad (6)$$

For a nonpowered swing-by to be feasible, the periapsis radius must be higher than a minimum radius; that is, $r_{\text{per}} > r_{\text{permin}}$. In this work, we assumed $r_{\text{permin}} = 1.1R_p$. This value is suitable for most solar planets, as Earth and Venus. A much higher periapsis radius is used in Jupiter swing-by to avoid radiation effects. If the desired gravity assist is not feasible via a nonpowered swing-by, then an impulsive post-swing-by maneuver is applied (the powered swing-by). By applying a small impulse during the swing-by, higher deflection angles could be attained [8]. The powered swing-by impulse can be computed using Eq. (7):

$$\Delta \mathbf{v}_{\text{ps}} = (\mathbf{v}_{s/c}^{+})_{\text{req}} - (\mathbf{v}_{s/c}^{+})_{\text{nps}} \quad (7)$$

where $(\mathbf{v}_{s/c}^{+})_{\text{req}}$ is the required spacecraft heliocentric outgoing velocity vector, and $(\mathbf{v}_{s/c}^{+})_{\text{nps}} = \mathbf{v}_p - \mathbf{v}_{\infty}^{+}$.

The swing-by plane needs to be computed in order to calculate \mathbf{v}_{∞}^{+} . To define the swing-by plane, a rotation angle η is introduced [9]. The vector \mathbf{v}_{∞}^{+} is obtained from the vector \mathbf{v}_{∞}^{-} by performing two consecutive rotations (δ and η). The incoming relative velocity vector \mathbf{v}_{∞}^{-} is defined in the heliocentric inertial frame $\hat{I}\hat{J}\hat{K}$. A local frame $\hat{i}\hat{j}\hat{k}$ is defined such that the unit vector \hat{i} is in the direction of the incoming relative velocity vector; so

$$\hat{i} = \frac{\mathbf{v}_{\infty}^{-}}{\|\mathbf{v}_{\infty}^{-}\|} \quad (8)$$

The plane of the swing-by maneuver is the ij plane. Therefore, the outgoing relative velocity vector, as expressed in the local frame $(\mathbf{v}_{\infty}^{+})_L$, is

$$(\mathbf{v}_{\infty}^{+})_L = v_{\infty} [\cos \delta \quad \sin \delta \quad 0]^T \quad (9)$$

The \mathbf{v}_{∞}^{+} is computed in the inertial frame via a coordinate transformation from the local frame to the inertial frame, as shown in Fig. 4. To perform this transformation, the following procedures are applied. The perpendicular plane Π defined by its normal \hat{i} intersects with the inertial ecliptic plane (IJ plane) in the line Γ . The direction of Γ depends on the orientation of the incoming relative velocity in

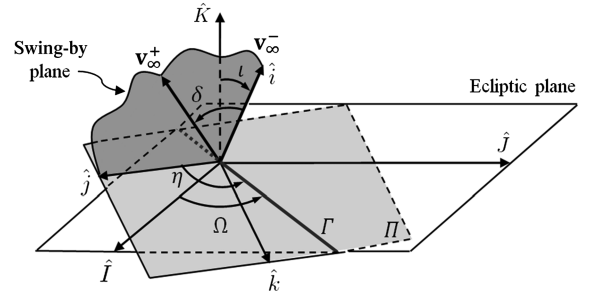


Fig. 4 Transformation scheme from local frame ijk to inertial frame IJK , showing definition of rotation angle η .

the inertial frame. The angle between Γ and the inertial \hat{I} is Ω , which is defined in the IJ plane. The angle between Γ and the unit vector \hat{j} is the rotation angle η , which is defined in the perpendicular plane Π . The inclination of plane Π to the ecliptic plane is ι . A three-angle rotation is performed to calculate the local unit vector \hat{j} in the inertial frame according to the following relation:

$$\hat{j} = \begin{bmatrix} \cos(-\Omega) & \sin(-\Omega) & 0 \\ -\sin(-\Omega) & \cos(-\Omega) & 0 \\ 0 & 0 & 1 \end{bmatrix} \begin{bmatrix} 1 & 0 & 0 \\ 0 & \cos(-\iota) & \sin(-\iota) \\ 0 & -\sin(-\iota) & \cos(-\iota) \end{bmatrix} \times \begin{bmatrix} \cos(-\eta) & \sin(-\eta) & 0 \\ -\sin(-\eta) & \cos(-\eta) & 0 \\ 0 & 0 & 1 \end{bmatrix} \begin{bmatrix} 1 \\ 0 \\ 0 \end{bmatrix} \quad (10)$$

Finally, the outgoing velocity vector in the inertial frame is computed as follows:

$$\mathbf{v}_{\infty}^{+} = C(\mathbf{v}_{\infty}^{+})_L \quad (11)$$

where C is the transformation matrix:

$$C = [\hat{i} \quad \hat{j} \quad \hat{k}] \quad (12)$$

C. N -Impulses Multi-Gravity-Assist Trajectory

In this section, a formulation is introduced for the full problem of optimal trajectory design, including MGA maneuvers and, possibly, N -impulses in each leg. The mission is designed to transfer a spacecraft from a departure planet P_d to a target (arrival) planet P_a . Time windows are given for each of the departure and arrival dates. Consider a mission that consists of m gravity-assist maneuvers. There are $m + 1$ different legs in the trajectory. Each leg contains n_l DSMs. The TOF for each leg, except the last leg, is an independent design variable. The calculations of the dependent variables are carried out starting from the departure planet, from one leg to the next, and so on.

In any trajectory leg, the spacecraft trajectory is solved as discussed in Sec. III.A. The velocity vector at the leg endpoint is the heliocentric incoming velocity vector of the consequent gravity-assist maneuver. If a leg has at least one DSM, then the swing-by maneuver at the beginning of that leg is assumed a nonpowered swing-by maneuver. The swing-by independent design variables are the pericenter altitude h and the rotation angle η . The swing-by maneuver calculations are carried out, as discussed in Sec. III.B, to yield the outgoing spacecraft velocity vector. This velocity vector is the spacecraft heliocentric velocity vector of the initial point on the consequent transfer trajectory. The process is repeated for all legs and swing-by maneuvers.

If any of the swing-by maneuvers is followed by a leg with no DSM, then that swing-by is assumed to be a powered swing-by maneuver. In this case, all dependent variables associated with the leg before the swing-by are calculated first. Then, the dependent variables associated with the leg after the powered swing-by are computed. Finally, the powered swing-by variables, including the

swing-by impulse, are computed such that the two leg calculations are compatible. Assume the powered swing-by planet is planet P_l . The leg before planet P_l is leg l , and the leg after it is leg $l + 1$. The times of swinging by planets P_l and P_{l+1} are known; hence, the positions of the spacecraft at these two times are known. There is no DSM in leg $l + 1$; hence, a Lambert's problem is solved to calculate the spacecraft velocity vectors on the initial and final points of leg $l + 1$. The velocity vector at the initial point of leg $l + 1$ is the required heliocentric outgoing velocity vector $(\mathbf{v}_{s/c}^+)_{\text{req}}$ of the powered swing-by at planet P_l . To achieve this velocity, a swing-by impulse $\Delta \mathbf{v}_{\text{ps}}$ is added. Since it is desired to achieve all maneuvers with minimum fuel. We assume that the powered swing-by maneuver plane is the plane containing the incoming relative velocity vector \mathbf{v}_{∞}^- and the required outgoing relative velocity vector $(\mathbf{v}_{\infty}^+)_{\text{req}}$ so that $\Delta \mathbf{v}_{\text{ps}}$ does not have an out-of-plane component:

$$(\mathbf{v}_{\infty}^+)_{\text{req}} = (\mathbf{v}_{s/c}^+)_{\text{req}} - \mathbf{v}_p \quad (13)$$

Equations (6), (7), and (13) are used to calculate $\Delta \mathbf{v}_{\text{ps}}$. The required deflection angle δ_{req} between \mathbf{v}_{∞}^- and $(\mathbf{v}_{\infty}^+)_{\text{req}}$ is computed as

$$\delta_{\text{req}} = \cos^{-1} \left(\frac{\mathbf{v}_{\infty}^- \cdot (\mathbf{v}_{\infty}^+)_{\text{req}}}{\|\mathbf{v}_{\infty}^-\| \|(\mathbf{v}_{\infty}^+)_{\text{req}}\|} \right) \quad (14)$$

The maximum deflection angle δ_{max} is calculated from Eq. (5) by substituting r_{per} with the permissible minimum periapsis radius r_{permin} . If $\delta_{\text{req}} \leq \delta_{\text{max}}$, then \mathbf{v}_{∞}^+ is in the same direction as $(\mathbf{v}_{\infty}^+)_{\text{req}}$ and is calculated as

$$\mathbf{v}_{\infty}^+ = \mathbf{v}_{\infty}^- \frac{(\mathbf{v}_{\infty}^+)_{\text{req}}}{\|(\mathbf{v}_{\infty}^+)_{\text{req}}\|} \quad (15)$$

If $\delta_{\text{req}} > \delta_{\text{max}}$, then δ_{max} is used, and the swing-by maneuver is carried out in the same plane defined by \mathbf{v}_{∞}^- and $(\mathbf{v}_{\infty}^+)_{\text{req}}$.

IV. Optimization

The independent design variables to be optimized are described in Sec. II. In this paper, the objective is to minimize the total cost Δv_T of the trajectory for a MGADSM mission that consists of m gravity-assist maneuvers and n_l DSMs in each leg of the $m + 1$ mission legs. Equation (16) shows the total cost of the mission:

$$\Delta v_T = \|\Delta \mathbf{v}_d\| + \sum_1^m \|\Delta \mathbf{v}_{\text{ps}}\| + \sum_1^{m+1} \sum_1^{n_l} \|\Delta \mathbf{v}_{\text{DSM}}\| + \|\Delta \mathbf{v}_a\| \quad (16)$$

where $\Delta \mathbf{v}_d$ and $\Delta \mathbf{v}_a$ are the departure and arrival impulses, respectively, $\Delta \mathbf{v}_{\text{ps}}$ is the post-swing-by impulse of the powered gravity assist only, and $\Delta \mathbf{v}_{\text{DSM}}$ is the applied DSM impulse. The fitness F at a design point, which is maximized to determine the fittest solution, is defined as

$$F = \frac{1}{\Delta v_T} \quad (17)$$

A GA is adopted for optimization to find the most fit solutions. Each individual design point in the GA population represents a set of independent design variables. Those variables are divided into two categories: discrete and continuous variables, as seen in Table 1. Each individual is presented in a binary format as a binary string. This string contains the binary representation of all the design variables values at the corresponding design point. The number of bits for each variable determines its accuracy. For the continuous design variables (CDVs), the number of bits q_A for a CDV A is selected according to the following inequality:

$$2^{q_A} \leq \frac{A_{\text{max}} - A_{\text{min}}}{\Delta_A} + 1; \quad A_{\text{max}} \neq A_{\text{min}} \quad (18)$$

where A_{min} and A_{max} are the lower and upper bounds of the variable A , and Δ_A is the desired accuracy of A . For the DDVs, each variable would be assigned a unique binary string. The number of bits q_B for a

Table 1 Discrete and continuous independent design variables of the MGADSM problem

DDVs	CDVs
Number of swing-by maneuvers, m	Departure date, t_d
Swing-by planets, P_1, \dots, P_i	Arrival date, t_a
Count of DSMs in each leg, n_1, \dots, n_{i+1}	TOF, T_1, \dots, T_i
Flight direction, f	Normalized pericenter altitudes, $\bar{h}_1, \dots, \bar{h}_i$
	Rotation angles, η_1, \dots, η_i
	Epochs of DSMs, $\varepsilon_1, \dots, \varepsilon_j$
	DSMs, $\Delta \mathbf{v}_1, \dots, \Delta \mathbf{v}_k$

DDV B depends on the lower and upper bounds of the variable, B_{min} and B_{max} , respectively. The variable q_B is computed as

$$q_B = 1 \text{ bit} \quad \text{if } B_{\text{max}} = B_{\text{min}} \quad (19)$$

or

$$2^{q_B} \leq B_{\text{max}} - B_{\text{min}} + 1 \quad \text{if } B_{\text{max}} \neq B_{\text{min}}$$

In Table 1, i is the maximum possible number of swing-by maneuvers and j is the maximum possible number of total DSMs in the entire trajectory (both i and j are specified by the user). The term DSM is used to define any thrust impulse applied during the mission course, except the launch, arrival, and powered swing-by impulses. The maximum number of independent thrust impulses is k , which can be explained as follows: if n_l is the maximum number of DSMs in a leg, then there are n_l independent thrust impulses if this leg is the first one; while for the consequent legs, the number of required independent thrust impulses is $n_l - 1$. Each thrust impulse $\Delta \mathbf{v}$ consists of three CDVs. The pericenter altitudes h are normalized with respect to the mean radius of the associated swing-by planet, R_p . The normalized pericenter altitudes \bar{h} are used as design variables to limit the resulting pericenter altitudes to feasible values only when dealing with different swing-by planets with obvious varied radii. The epoch of a DSM ε specifies the time at which the impulsive maneuver is applied as a fraction of the associated leg transfer time. For most applications, a DSM could be applied from 10 up to 90% of the total TOF in the associated leg. The flight direction f of the whole mission is either retrograde or prograde.

Given that the maximum possible number of swing-by maneuvers is i , then we create i DDVs P_1, P_2, \dots, P_i . Each variable P_l determines the planet about which the l th swing-by occurs, as shown in Fig. 5. The range of the discrete variable P_l is one through eight, which are the indices for the planets in the solar system, from Mercury to Neptune. The order of the swing-bys is the same as the order of the variables P_l , as shown in Fig. 5. If the selected number of swing-bys is $m < i$, then the first m variables (P_1, P_2, \dots, P_m) will be selected.

For a MGADSM problem, the total number of independent design variables depends on the number of swing-by maneuvers m and the number of DSMs in every leg, n_1, \dots, n_{i+1} . Selecting different values for the DDVs, m, n_1, \dots, n_{i+1} , changes the mission scenario and the number of DSMs in each leg. So, for a given solution, the values of these variables dictate the length of a certain portion in the chromosome of that solution. For example, if $m = 2$, then we need to allocate two swing-by portions in the chromosome; however, if $m = 3$, then three positions will be needed for swing-bys in the chromosome. Thus, changing the mission scenario and/or the number of DSMs is accompanied by a change in the length of the

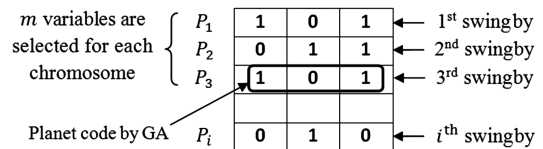


Fig. 5 Coding of swing-by planets.

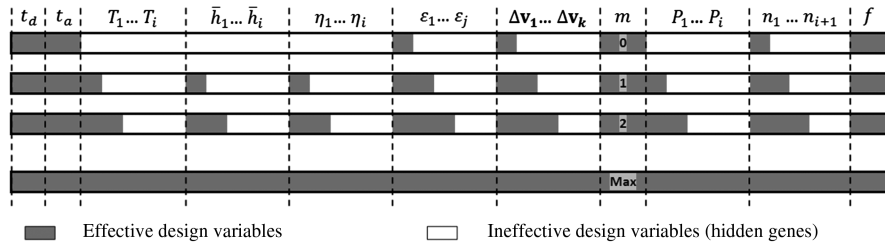


Fig. 6 Typical chromosomes for trajectory optimization problem; each row represents a chromosome.

chromosome. Standard GAs cannot handle this problem because of the variation of string lengths among different solutions. Genetic operations, such as crossover, are defined only for fixed-length string populations. To overcome this problem, the concept of hidden genes is introduced.

Let L_{\max} be the length of the longest possible chromosome (this chromosome corresponds to a trajectory in which the spacecraft performs the maximum possible number of swing-bys and applies the maximum number of DSMs). All chromosomes in the population are allocated a fixed length equal to L_{\max} , which is computed based on the design variables stated in Table 1, as in Eq. (20):

$$L_{\max} = 5 + 3i + j + 2(i - z) + 3k \quad (20)$$

where z is the number of swing-by maneuvers that are followed by a no-impulse leg. From the upper bounds of the key design variables (m, n), the maximum chromosome length could be calculated a priori. In a general solution (a point in the design space), some of the variables in the chromosome will be ineffective in cost function evaluation; the genes describing these variables are here referred to as hidden genes. The hidden genes, however, will be used in the genetic operations in generating future generations. Figure 6 shows typical solution chromosomes, where the variables at the top of the figure are the independent design variables. Each row in Fig. 6 represents a member (single individual) in the GA population. The dark parts represent genes that are effective in fitness function evaluations. The white parts represent the hidden genes.

Because all chromosomes have the same length, standard definitions of GAs operations can still be applied to this problem. Hidden genes will take part in all genetic operations like normal genes. To illustrate this concept, an example on the crossover operation between two parent solutions to generate two children (new) solutions is presented here. Figure 7 shows two parent chromosomes and the resulting chromosomes after crossover, where a single point crossover is performed. Consider, for example, the genes representing the number of swing-by maneuvers and the genes representing the number of DSMs. The genes representing the number of swing-bys and the numbers of DSMs are always effective genes. The chromosome length allows for up to five swing-bys and up to two DSMs in each leg. In the first parent, the genes representing the first two swing-bys are effective genes, while there are hidden genes representing the other three swing-bys.

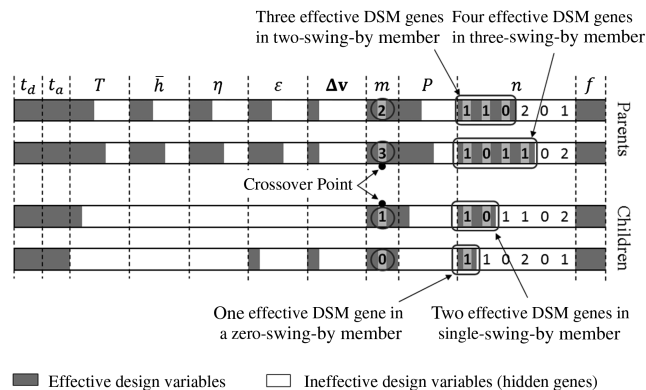


Fig. 7 Crossover operation.

Similarly, the genes representing the numbers of DSMs of legs 1 through 3 (n_1-n_3) are effective genes, while there are hidden genes representing the rest of DSMs variables. In the second parent, the genes representing the first three swing-bys are effective genes, while the genes representing the other two swing-bys are hidden. The genes representing the first four DSM variables are effective genes (n_1-n_4), while there are hidden genes representing the rest of DSM variables. The crossover operation is carried out as defined in the standard GA. The resulting two children are shown in Fig. 7. The first child has effective genes representing a single swing-by and two DSM variables. The effective genes in the second child correspond to a zero-swing-by maneuver with a single DSM maneuver. The rest of the chromosomes of the children are hidden genes that represent the ineffective design variables. Therefore, the generated children could have different scenarios and DSM sequences from those of the origin parents.

This algorithm is tested for several interplanetary missions, ranging from simple to complex missions. The optimization algorithm (ITO-HGGA tool) is designed to find the mission scenario (the number of swing-bys and the planets to swing by) as well as the rest of the independent design variables: the times of swing-by, the number of DSMs, the times of DSMs, the magnitudes/directions of DSMs, and the departure/arrival dates. The size of the design space is controlled by the bounds of the independent design variables.

To reduce the computational cost for complex missions, the problem may be solved by a two-phase approach. A trajectory design optimization can be started by assuming no DSMs in the trajectory (zero-DSM trajectory). This reduces the number of independent design variables by eliminating the following design variables: periapsis altitudes, rotation angles, epoch of DSMs, and thrust impulses. This reduction in the number of design variables allows for exploring wider ranges for each of the remaining design variables. Specifically, we can open the search space for any number of swing-bys with any planets in the solar system; wider ranges of departure and arrival dates and times of flight can be used, and both possible flight directions can be considered. This will result in a set of fit scenarios (zero-DSM solutions). For each one of these scenarios, we then allow DSMs to be added to the trajectory and optimize our selection for these DSMs. So, we optimize on the number of DSMs in each leg and their locations/magnitudes/directions while maintaining the fixed scenario. The departure/arrival dates and TOFs are allowed to change as design variables, with narrow ranges around the values obtained from the zero-DSM solution. This technique of solving the problem by the two-phase approach has the advantage of reducing the computational time. This reduction in computational time comes at a price; most of the design space will not be explored. In general, optimizing a given scenario through adding DSMs improves the fitness of this trajectory (if a zero-DSM trajectory is optimal, then the second step in the optimization process will add no DSMs to the scenario). On the other hand, some solutions are fit only when there are DSMs in the trajectory and the fitness of the corresponding zero-DSM scenario is poor [e.g., the Mercury Surface, Space Environment, Geochemistry, and Ranging (MESSENGER) mission trajectory is fit when we have a DSM in the first leg and becomes poor if we assume no DSM in the first leg]. This means that it is not possible to find the zero-DSM solution among the fittest solutions in the first step. For this kind of trajectory, it is not possible to find the optimal solution by solving the problem using the two-phase approach.

Table 2 Bounds of design variables for EM mission

Design variables	Lower bound	Upper bound
Number of swing-by maneuvers, m	0	2
Swing-by planets identification numbers, P_1, \dots, P_i	1 (Mercury)	8 (Neptune)
Number of DSMs in each mission leg, n_1, \dots, n_{i+1}	0	2
Flight direction, f	Posigrade	Retrograde
Departure date, t_d	01 June 2004	01 July 2004
Arrival date, t_a	01 April 2005	01 July 2005
TOF, days/leg; T_1, \dots, T_i	40	300
Swing-by normalized pericenter altitude, $\bar{h}_1, \dots, \bar{h}_i$	0.1	10
Swing-by plane rotation angle, rad; η_1, \dots, η_i	0	2π
Epoch of DSM, $\varepsilon_1, \dots, \varepsilon_j$	0.1	0.9
DSM, km/s; $\Delta \mathbf{v}_1, \dots, \Delta \mathbf{v}_k$	-5	5

As an example, consider the Cassini 2 mission trajectory: let the maximum possible number of swing-by maneuvers be four, and let only one impulse, as a maximum, be applied in each leg. In optimizing all the design variables, the required number of independent design variables is 33 (11 DDVs and 22 CDVs). This is a computationally expensive problem, especially with wide ranges for the design variables. On the other hand, by solving a zero-DSM problem, the number of design variables is reduced to only 12 variables (six DDVs and six CDVs). This step solves for the optimum mission scenario without DSMs. Then, the second step is performed with 27 design variables (five DDVs and 22 CDVs). The ranges of the CDVs in the second step are reduced based on the information from the initial mission scenario.

The ITO-HGGA tool also optimizes the number of revolutions in each leg. The TOF of each leg and the time of applying each DSM are selected as design variables to allow for multirevolution transfers. Lambert's problem is solved once in each leg. Based on the position vectors and the TOF, Lambert's solution may have both single-revolution and multirevolution transfers. The selection criterion is as follows: the selected Lambert's transfer should minimize the former maneuver cost. This maneuver could be a departure impulse, a DSM, or a swing-by maneuver. In the final leg, the selected Lambert's transfer will minimize the former maneuver cost plus the arrival impulse cost.

A MATLAB toolbox (GENETIC v2.1) is used [27]. GENETIC v2.1 is structured such that continuous, discrete, and mixed continuous/discrete problems can be addressed. The main operations in the basic GA are coding, evaluation, selection, crossover, and mutation. GA tuning parameters depend on the specific problem. A uniform crossover operation is conducted with a probability varied from 0.9 to 0.98. The mutation probability is selected between 0.01 and 0.08. A roulette wheel is used in the selection operation. Proportional ranking is implemented in most cases. In general, linear ranking is implemented with higher crossover probability values, in solving a zero-DSM problem, in order to increase the diversity in the population. The linear ranking is implemented to avoid local minima traps. To maintain a diverse population, a niching principle is applied by degrading the fitness of

Table 3 MGADSM solution trajectory for the EVM mission

Mission parameter	MGADSM scenario
Departure date, t_d	05 June 2004 00:28:38
Departure impulse, km/s	4.53
DSM date	11 Sept. 2004 18:35:44
DSM impulse, km/s	$0.1293 (t_d + 98.77 \text{ days})$
Venus swing-by date	19 Nov. 2004 01:42:40
Post-swing-by impulse, km/s	2.27×10^{-12}
Pericenter altitude, km	7937.913
Arrival date	15 May 2005 15:07:38
Arrival impulse, km/s	6.095
TOF, days	167.07, 177.6
Mission duration, days	344.67
Mission cost, km/s	10.754

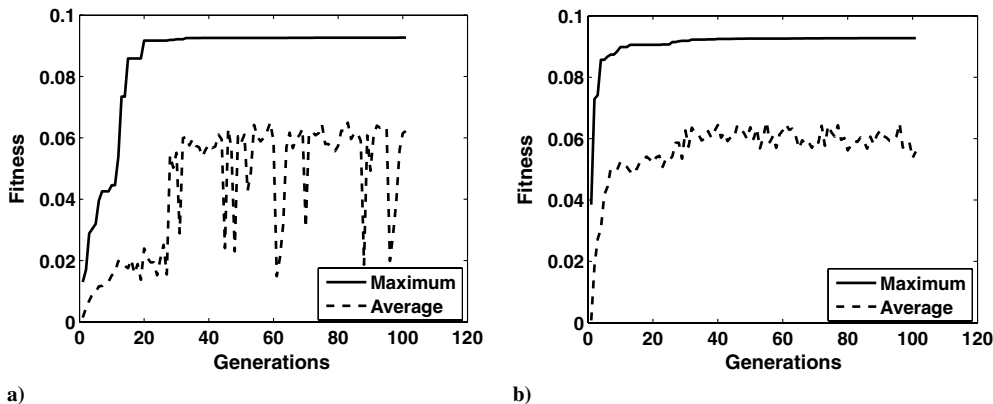
the similar individuals [28]. A simple niching technique is implemented to solve the complex case of the Cassini 2 mission. The fittest solution obtained by the GA is not necessarily an optimal solution, nor is it at a local minimum. Therefore, a constrained nonlinear optimization technique is used to improve the solution by finding the closest local minimum to that solution. The local optimizer is only optimizing over the CDVs, not the discrete variables. The GA solution is used as an initial guess in the local search algorithm.

V. Numerical Results

This section presents a number of case studies for interplanetary space mission trajectory optimization. Comparisons to other solutions in the literature are presented to validate the obtained results.

A. Earth-Mars Mission

A MGADSM trajectory is optimized for the EM mission. The lower and upper bounds for all design variables are listed in Table 2. The maximum possible number of swing-by maneuvers is selected to

**Fig. 8** Convergence of optimization algorithm for EVM mission: a) zero-DSM model and b) MGADSM model.

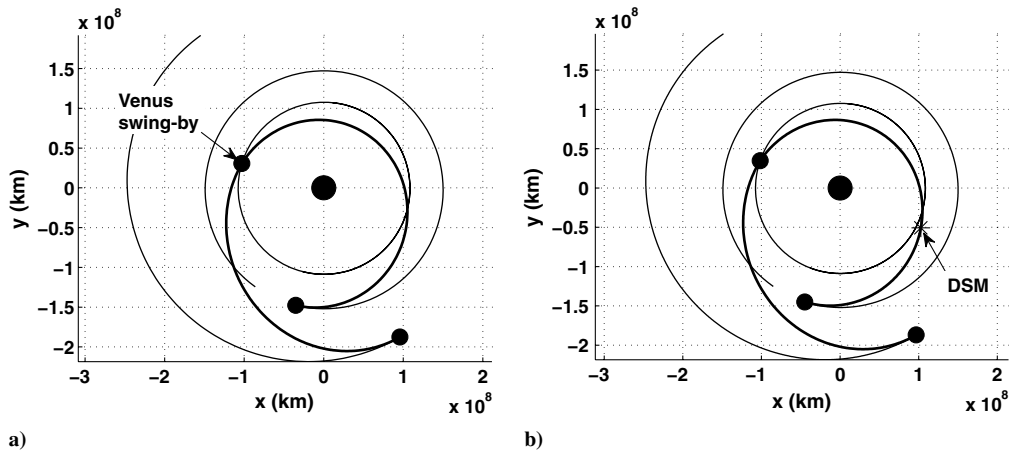


Fig. 9 Optimal EVM mission: a) zero-DSM model and b) MGADSM model.

be two. The maximum number of DSMs in each leg is selected to be two impulses. As can be seen from Table 2, a gravity-assist maneuver could be performed with any planet in the solar system, from Mercury to Neptune. The direction of flight can be posigrade or retrograde. The TOF of each leg, except the last one, is selected between 40 and 300 days.

The total number of design variables for this mission is 33 (seven DDVs and 26 CDVs). Wide ranges for the design variables are adopted, as listed in Table 2. A population of 500 individuals is used for 300 generations. A local optimizer uses the fittest GA solution as an initial guess to find a local minimum. The resulting solution has a single swing-by maneuver at Venus, with a total cost of 10.754 km/s. The fittest trajectory has a single DSM in the first leg, as shown in Table 3.

The same problem is solved again by dividing the optimization process into two steps to reduce the required computational time. First, a zero-DSM solution is sought to determine a mission scenario. The number of design variables in this first step is only eight

variables. ITO-HGGA, with 200 populations and 100 generations, is used. The convergence of the optimization algorithm is shown in Fig. 8. The resulting zero-DSM scenario is a single swing-by maneuver at Venus with a cost of 10.788 km/s. Then, the local optimization tool is used to improve the solution to the nearest local minimum solution. The local optimizer reduces the cost to 10.783 km/s. A powered swing-by is implemented in this case, and the required impulse of the swing-by is 0.002 km/s. Figure 9 shows the zero-DSM Earth–Venus–Mars (EVM) trajectory.

In the second step, the problem is solved using the full MGADSM formulation, assuming that the mission scenario is EVM (the scenario obtained from the first step). The ranges for the departure, swing-by, and arrival dates are varied within only 10 days around those values obtained from the first step. The number of design variables in this step is 12 (two DDVs and 10 CDVs). A population of 300 individuals has been used for 100 generations of GAs followed by a local minima optimizer. The result of the second optimization step is a single DSM of 180.1 m/s in the first leg at 80.81 days from

Table 4 MGADSM solution trajectory for EVM mission using two-phase approach technique

Mission parameter	Zero-DSM model initial estimate	MGADSM model final scenario
Departure date, t_d	05 June 2004 01:52:21	02 June 2004 11:43:25
Departure impulse, km/s	4.616	4.457
DSM date	—	22 Aug. 2004 00:07:46
DSM impulse, km/s	—	0.1801 ($t_d + 80.81$ days)
Venus swing-by date	20 Nov. 2004 15:10:59	19 Nov. 2004 07:02:55
Post-swing-by impulse, km/s	0.002	1.68×10^{-13}
Pericenter altitude, km	7996.782	7869.048
Arrival date	14 May 2005 13:18:06	16 May 2005 03:29:08
Arrival impulse, km/s	6.165	6.091
TOF, days	168.56, 174.92	169.81, 177.85
Mission duration, days	343.48	347.66
Mission cost, km/s	10.783	10.728

Table 5 Bounds of Earth–Jupiter mission design variables

Design variables	Lower bound	Upper bound
Number of swing-by maneuvers, m	0	2
Swing-by planets identification numbers, P_1, \dots, P_i	1 (Mercury)	8 (Neptune)
Number of DSMs in each mission leg, n_1, \dots, n_{i+1}	0	2
Flight direction, f	Posigrade	Retrograde
Departure date, t_d	01 Sept. 2016	30 Sept. 2016
Arrival date, t_a	01 Sept. 2021	31 Dec. 2021
TOF, days/leg; T_1, \dots, T_i	80	800
Swing-by normalized pericenter altitude, $\bar{h}_1, \dots, \bar{h}_i$	0.1	10
Swing-by plane rotation angle, rad; η_1, \dots, η_i	0	2π
Epoch of DSM, $\varepsilon_1, \dots, \varepsilon_j$	0.1	0.9
DSM, km/s; $\Delta v_1, \dots, \Delta v_k$	−5	5

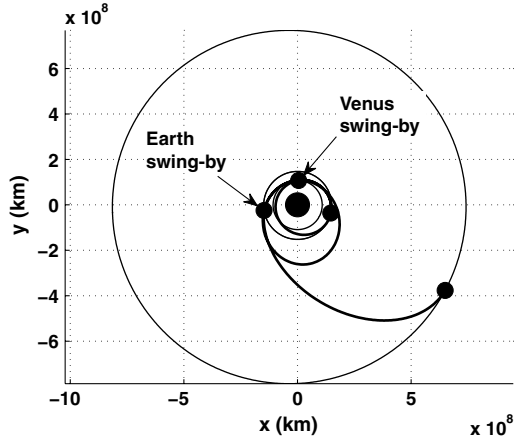


Fig. 10 Optimal zero-DSM trajectory of Earth-Jupiter mission.

mission start time, as shown in Fig. 9. The total transfer cost is slightly reduced to 10.728 km/s in the second optimization step. Table 4 shows the zero-DSM trajectory, as well as the final trajectory. As shown in Table 4, the effect of the DSM is reducing the departure and arrival impulses, as well as reducing the impulse of the powered swing-by, to almost zero. The fittest trajectory could be considered as a nonpowered gravity-assist trajectory with a single DSM.

B. Earth-Jupiter Mission

A mission to Jupiter is considered. It is desired to find the MGADSM trajectory with minimum cost. Wide ranges of all design variables are allowed in optimization to explore more of the design space. The design variable bounds are listed in Table 5. The total number of design variables is 33 (seven DDVs and 26 CDVs). The zero-DSM model is used to determine an initial scenario. The independent design variables in this step are eight variables (four DDVs and four CDVs). A population of 300 individuals and 100 generations are used in GA optimization. The resulting fittest scenario is a two-swing-by trajectory with swing-bys around Venus and then Earth [Earth-Venus-Earth-Jupiter (EVEJ)], as shown in Fig. 10. The solution is a posigrade multirevolution trajectory. The total cost of this zero-DSM trajectory is 10.298 km/s, as shown in Table 6. The scenario of this solution is then used in the second optimization step. The two swing-bys are fixed (EVEJ). The departure/arrival dates and the TOF design variables obtained from the first step are allowed to vary within 10 days from their values obtained from the first step. A population of 500 individuals and 100 generations is used. Figure 11 shows the convergence of the

optimization algorithm. Table 6 shows the zero-DSM solution, as well as two solutions with DSMs. One solution has a single DSM in the second leg (Venus-Earth), while the other solution has a single DSM in the first leg [Earth-Venus (EV)], as shown in Fig. 12. In the first scenario, the DSM amplitude is 0.2 m/s, which seems an insignificant value with respect to the total trajectory cost. It is expected that this small DSM may be vanished with more iterations.

C. Earth-Saturn Mission (Cassini 2)

One of the most complicated MGA trajectories is the Cassini 2 trajectory. In 1997, The Cassini-Huygens mission was launched to study the planet Saturn and its moons [11]. The ITO-HGGA tool is used to search for a minimum-cost trajectory for an Earth-Saturn trip. For the sake of making comparisons with the literature, a narrow range of departure dates is allowed around the known published date for the Cassini 2 mission. The ranges for the other design variables are wide enough to investigate all possible solutions. Table 7 presents the upper and lower bounds for the design variables. A zero-DSM model is initially used to find an initial mission scenario. There are 12 independent design variables in this step (six DDVs and six CDVs). A population of 500 individuals and 1500 generations is used. Initial attempts show that resulting solutions are always trapped in regions that are worse than the known solutions for the Cassini 2 mission. This suggests allowing more time (more generations) for ITO-HGGA to search for more solutions. To avoid high computational costs, a simple niching technique is implemented [28]. The GA convergence is shown in Fig. 13.

The obtained mission scenario is a four-swing-by trajectory with the same planet sequence as the actual Cassini 2 mission scenario [Earth-Venus-Venus-Earth-Jupiter-Saturn (EVVEJS)]. The trajectory is a posigrade transfer with 10.685 km/s total transfer cost, as shown in Table 8. Then, the initial zero-DSM scenario is used in the MGADSM model to obtain the final trajectory. The planet sequence is fixed at EVVEJS, with narrow ranges for the departure, arrival, and gravity-assist dates. A population of 500 individuals and 1000 generations is used. Then, a local optimizer is used. Twenty-seven design variables are used in this model (five DDVs and 22 CDVs). The GA convergence is shown in Fig. 13. The final solution is presented in Table 8. The trajectory has two DSMs, one in the first leg (EV) and the other is in the second leg (Venus-Venus). The total transfer cost is reduced to 8.385 km/s after applying the DSMs. The zero-DSM initial trajectory and the MGADSM final trajectory are shown in Fig. 14.

VI. Discussion

The cost being optimized in this work is a function of discrete and CDVs. The discrete variables determine the mission scenario

Table 6 Optimal MGADSM trajectory of EVEJ mission

Mission parameter	Zero-DSM model initial estimate	MGADSM Model	
		Scenario (1)	Scenario (2)
Departure date	09 Sept. 2016 11:38:03	06 Sept. 2016 13:36:17	07 Sept. 2016 01:55:17
Departure impulse, km/s	3.653	3.542	3.439
DSM date	—	—	21 Feb. 2017 08:29:43
DSM impulse, km/s	—	—	0.109
Venus swing-by date	05 Sept. 2017 05:57:07	05 Sept. 2017 14:57:28	07 Sept. 2017 07:43:57
Post-swing-by impulse, km/s	0.0004	—	2.38e - 014
Pericenter altitude, km	1402.2	1307.28	613.545
DSM date	—	14 May 2018 09:31:08	—
DSM impulse, km/s	—	0.0002	—
Earth swing-by date	30 March 2019 02:25:00	30 March 2019 03:14:06	29 March 2019 02:19:05
Post-swing-by impulse, km/s	0.443	0.441	0.444
Pericenter altitude, km	637.8	637.8	637.8
Arrival date	18 Sept. 2021 21:15:27	24 Sept. 2021 23:59:59	17 Sept. 2021 07:43:51
Arrival impulse, km/s	6.202	6.195	6.19
TOF, days	360.76, 570.85, 903.79	364.05, 570.51, 909.87	365.24, 567.77, 903.23
Mission duration, days	1835.4	1844.43	1836.24
Mission cost, km/s	10.298	10.178	10.182

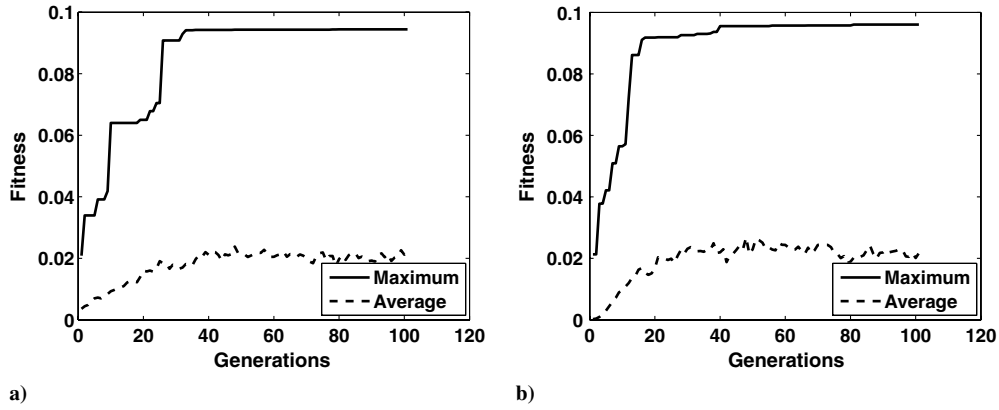


Fig. 11 Convergence of optimization algorithm of Jupiter mission: a) zero-DSM model and b) MGADSM model.

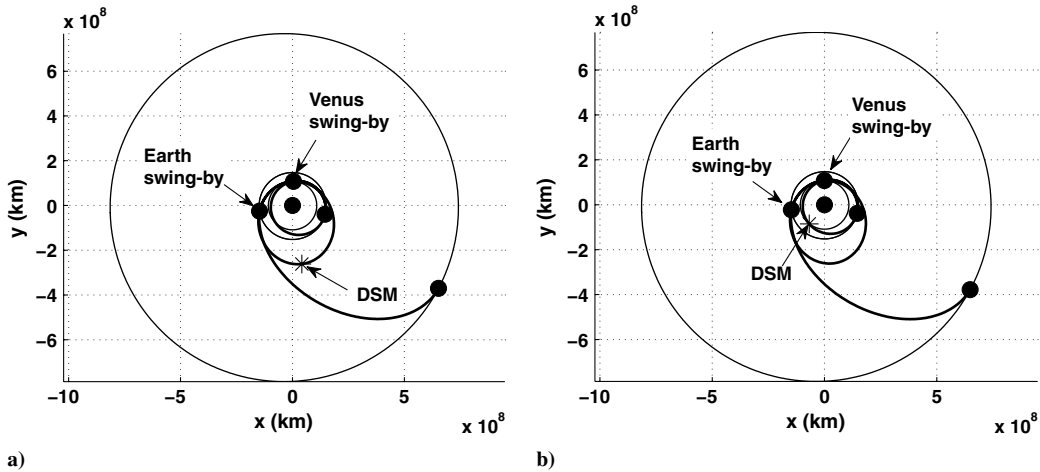


Fig. 12 Optimal EVEJ mission: a) case 1 (10.178 km/s) and b) case 2 (10.182 km/s).

(swing-by planets), the number of DSMs in each leg, and the direction of flight (posigrade and retrograde). The continuous variables determine the dates and parameters of the events. The ITO-HGGA tool implemented in this paper finds the values for all the design variables in the best solution trajectory. Then, the mission scenario, the direction of flight, and the number of DSMs are fixed, and the continuous variables are tuned by a local optimizer. The local optimizer implements a constrained nonlinear optimization technique. The proposed hidden genes concept is different from the VCL-GA concept presented in [21]. The VCL-GA assumes the same size for all chromosomes in a given population. The chromosome length, however, may vary from one generation to another. On the other hand, the proposed hidden genes concept handles problems where chromosomes of different lengths may exist in the same population.

The EVM mission trajectory optimization has been addressed in the literature [7]. The solution presented in [7] was obtained using the

extended primer vector theory, and it has a single swing-by maneuver and a single DSM. In implementing the primer vector method, the departure and arrival dates were assumed fixed (the mission duration is 340 days). The Venus swing-by time was also constrained to occur at 165 days from departure. The resulting solution has a DSM of 68.7 m/s in the first leg at 96.08 days from mission start date. The total cost of the mission is 10.786 km/s [7]. The solution obtained using the ITO-HGGA tool in this paper has also one swing by Venus and one DSM of 180.1 m/s in the first leg at 80.81 days from launch date. The total cost of the mission is 10.728 km/s, as shown in Table 4. The reduction in the total cost obtained using the ITO-HGGA tool, as compared with that of [7], is accompanied by changes in the mission's launch, swing-by, and arrival dates, without significantly changing the total mission duration. This solution is obtained by allowing the maneuver's launch, swing-by, and arrival dates to be freely chosen during the zero-DSM optimization step.

Table 7 Bounds of Cassini 2 mission design variables

Design variables	Lower bound	Upper bound
Number of swing-by maneuvers, m	1	4
Swing-by planets identification numbers, P_1, \dots, P_i	2 (Venus)	5 (Jupiter)
Number of DSMs in each mission leg, n_1, \dots, n_{i+1}	0	1
Flight direction, f	Posigrade	Retrograde
Departure date, t_d	01 Nov. 1997	31 Nov. 1997
Arrival date, t_a	01 Jan. 2007	30 June 2007
TOF, days/leg; T_1, \dots, T_i	40	1000
Swing-by normalized pericenter altitude, $\bar{h}_1, \dots, \bar{h}_i$	0.1	10
Swing-by plane rotation angle, rad; η_1, \dots, η_i	0	2π
Epoch of DSM, $\varepsilon_1, \dots, \varepsilon_j$	0.1	0.9
DSM, km/s; $\Delta v_1, \dots, \Delta v_k$	-5	5

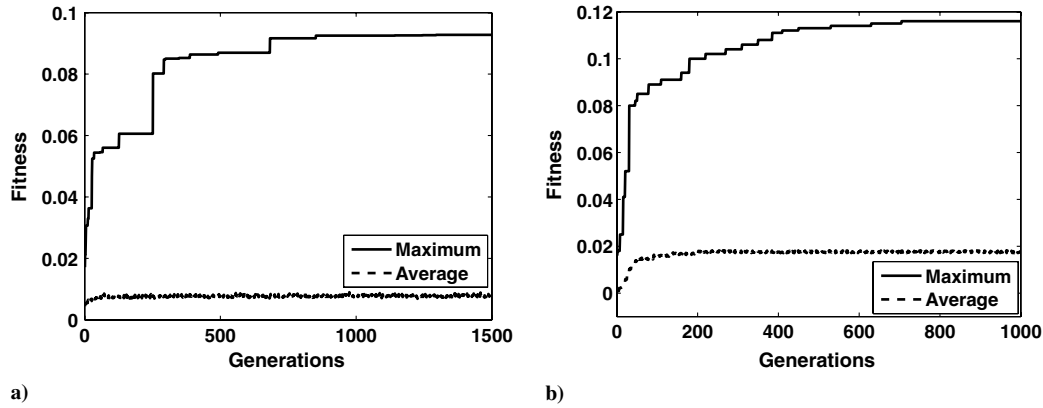


Fig. 13 Convergence of optimization algorithm of Cassini 2 mission: a) zero-DSM model and b) MGADSM model.

Reference [7] presents a minimum-cost solution trajectory for the Earth–Jupiter mission, assuming the fixed planet sequence EVEJ. The departure, arrival, and swing-by dates were also assumed fixed, with a launch in 2016 and a mission duration of 1862 days. The primer vector theorem solution has four DSMs. Two DSMs are applied in the first two legs. The total transfer cost for this solution is 10.267 km/s. The ITO-HGGA tool presented in this paper is able to automatically find the known swing-by sequence for the Jupiter mission in 2016. As listed in Table 6, the initial scenario (zero-DSM trajectory) is obtained, starting from wide ranges for the design variables. Then, the MGADSM solutions are obtained based on that initial scenario. Each of the two MGADSM solutions presented in Table 6 have less total cost than the solution presented in [7]. There is only one DSM in each of the two solutions. The solution presented in [7] requires four DSMs.

The Cassini 2 mission trajectory design problem has been addressed in several studies [7–10], where it is always assumed that a fixed swing-by sequence (EVVEJS) is known. In [9], the IMAGO obtained a solution that has a single DSM and a total cost of 9.06 km/s. Reference [7] implements the space pruning technique and finds the values and locations of the DSMs to minimize the total transfer cost. The departure, arrival, and swing-by dates were fixed. The minimum cost obtained in [7] is 8.877 km/s. Olympio and Izzo [8] recently developed an algorithm to find the optimal DSM

structure in a given trajectory scenario. For the Cassini 2 planet sequence described in the Global Trajectory Optimization Problems (GTOP) database [11], Olympio and Izzo [8] found a trajectory with a total cost of 8.387 km/s. The solution obtained using the ITO-HGGA tool in this paper finds a solution with a total cost of 8.385 km/s (as seen in Table 8), which is very close to the reported result in the GTOP database (8.383 km/s) [11], and it is also very close to the solution presented in [8]. The ITO-HGGA tool in this case, however, finds the planets sequence as well as the DSM structure.

Initially, the ITO-HGGA tool could not converge to the known planet sequence of the Cassini 2 mission in the first optimization phase. Rather, it converged to a worse solution. It has been observed that, in phase one, the solutions are trapped around a certain planet sequence that is worse than the known optimal scenario. The known optimal scenario (EVVEJS) could be obtained by forcing the last swing-by to be planet Jupiter. This suggested running the ITO-HGGA tool for more generations so that the optimal scenario is obtained. To avoid high computational cost and yet increase the diversity in the population, a niching algorithm is implemented [28]. A niching technique applies a fitness degradation to the row fitness function such that fitness is depressed in the regions where solutions have already been found [28]. In ITO-HGGA, a simple niching algorithm is added. Every five generations, the fitness is degraded for

Table 8 Optimal MGADSM trajectory of Cassini 2 mission

Mission parameter	Zero-DSM model initial estimate	MGADSM model final scenario
Departure date	30 Nov. 1997 00:00:00	13 Nov. 1997 11:12:37
Departure impulse, km/s	3.779	3.293
DSM date	—	25 March 1998 22:27:03
DSM impulse, km/s	—	0.449
Venus swing-by date	20 May 1998 12:58:21	30 April 1998 04:17:03
Post-swing-by impulse, km/s	2.633	—
Pericenter altitude, km	27,470.963	2590.174
DSM date	—	11 Dec. 1998 14:55:31
DSM impulse, km/s	—	0.396
Venus swing-by date	26 June 1999 14:04:56	27 June 1999 11:24:49
Post-swing-by impulse, km/s	1.096×10^{-05}	2.21×10^{-06}
Pericenter altitude, km	605.303	245.216
Earth swing-by date	19 Aug. 1999 09:05:31	19 Aug. 1999 16:18:04
Post-swing-by impulse, km/s	1.36×10^{-06}	6.04×10^{-08}
Pericenter altitude, km	1810.704	1975.905
Jupiter swing-by date	24 March 2001 00:21:22	31 March 2001 09:30:36
Post-swing-by impulse, km/s	1.89×10^{-04}	1.68×10^{-07}
Pericenter altitude, km	5,167,772.8	4,918,886.8
Arrival date	12 Jan. 2007 12:50:27	23 March 2007 21:31:17
Arrival impulse, km/s	4.273	4.247
TOF, days	171.54, 402.05, 53.79, 582.64, 2120.52	168.67, 423.3, 53.2, 589.72, 2182.54
Mission duration, days	3330.54	3417.43
Mission cost, km/s	10.685	8.385

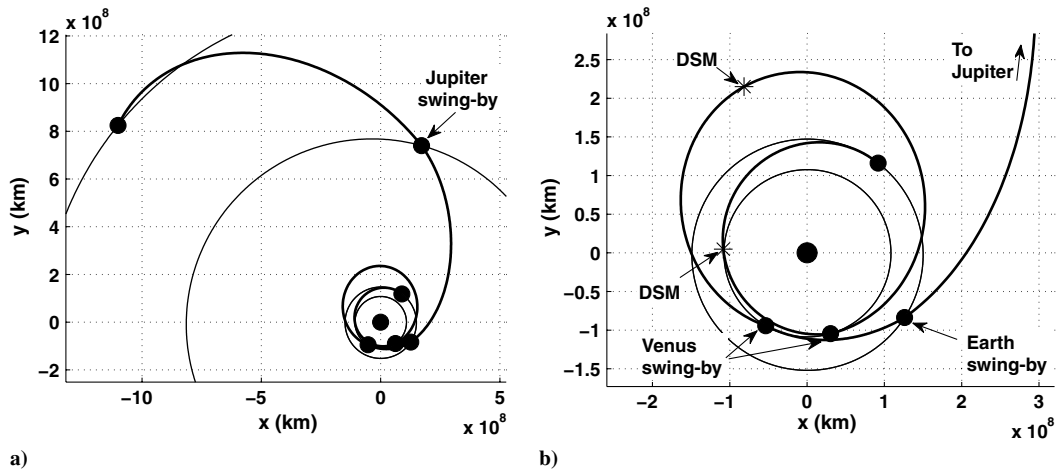


Fig. 14 Optimal Cassini 2 mission: a) zero-DSM model and b) MGADSM model (inner planets only).

the current fittest solution and all other solutions that have a similar planet sequence to the fittest solution. By implementing this niching technique, the ITO-HGGA tool is able to find the known optimal scenario in the first phase of optimization.

Figures 8, 11, and 13 show the convergence of the developed ITO-HGGA tool for the three case studies discussed in this paper. As can be seen from the figures, the number of generations needed for convergence to the solution varies from one case to another. In the EVM mission, 40 generations are needed in both the zero-DSM phase (eight design variables) and in the MGADSM phase (12 variables). In the Cassini 2 mission, the number of design variables is 12 and 27 for the first and the second phases, respectively. The zero-DSM phase converges in 900 generations, while the MGADSM phase converges in 700 generations. Therefore, the complex mission requires higher numbers of populations and generations than the simple mission to converge to the optimal solution.

VII. Conclusions

The interplanetary trajectory optimization (ITO) problem is addressed in this paper using a novel hidden genes optimization technique. The hidden genes algorithm has the capability to handle mixed (discrete and continuous) design variable optimization problems, with variable-sized design space. The concept of hidden genes genetic optimization proved capable of finding, without a priori knowledge, the number of swing-bys, the planets to swing by (optimal planet sequence), and the number of DSMs in each leg (as well as their components and directions), in addition to the rest of the design variables in the ITO problem. A fixed chromosome length is assumed for all chromosomes in the population. Part of the chromosome is effective in fitness function evaluations, while the other part (hidden genes part) is ineffective. Yet, the hidden genes take part in the genetic operations. In some problems, a niching technique is needed to increase the diversity in the population, and hence increases the speed of convergence. In the three case studies presented in this paper, the ITO-HGGA found the known optimal solutions, with improvements in some cases. To avoid long computational times, in some complex problems, a two-phase algorithm was implemented. The first phase finds only the mission scenario (planet sequence), while the second algorithm determines the DSM structure in the trajectory.

Acknowledgments

The authors would like to thank the Associate Editor and reviewers for their thorough review and feedback.

References

- [1] Wall, B. J., and Conway, B. A., "Genetic Algorithms Applied to the Solution of Hybrid Optimal Control Problems in Astrodynamics," *Journal of Global Optimization*, Vol. 44, No. 4, 2008, pp. 493–508. doi:10.1007/s10898-008-9352-4
- [2] Vasile, M., Minisci, E., and Locatelli, M., "Analysis of Some Global Optimization Algorithms for Space Trajectory Design," *Journal of Spacecraft and Rockets*, Vol. 47, No. 2, March–April 2010, pp. 334–344. doi:10.2514/1.45742
- [3] Battin, R. H., *An Introduction to the Mathematics and Methods of Astrodynamics*, AIAA, Reston, VA, 1987, pp. 419–470.
- [4] Navagh, J., "Optimizing Interplanetary Trajectories with Deep Space Maneuvers," NASA Langley Research Center, CR 4546, Hampton, VA, 1993.
- [5] Abilleira, F., "Broken-Plane Maneuver Applications for Earth to Mars Trajectories," 20th International Symposium on Space Flight Dynamics [CD-ROM], NASA, Sept. 2007.
- [6] Izzo, D., Becerra, V., Myatt, D., Nasuto, S., and Bishop, J., "Search Space Pruning and Global Optimisation of Multiple Gravity Assist Spacecraft Trajectories," *Journal of Global Optimization*, Vol. 38, No. 2, 2006, pp. 283–296. doi:10.1007/s10898-006-9106-0
- [7] Olympio, J. T., and Marmorat, J. P., "Global Trajectory Optimisation: Can We Prune the Solution Space when Considering Deep Space Maneuvers?," ARIADNA Final Rept. 06/4101, ESA, Sept. 2007.
- [8] Olympio, J. T., and Izzo, D., "Designing Optimal Multi-Gravity-Assist Trajectories with Free Number of Impulses," 21st International Symposium on Space Flight Dynamics, Toulouse, France, Sept. 2009.
- [9] Vasile, M., and Pascale, P. D., "Preliminary Design of Multiple Gravity-Assist Trajectories," *Journal of Spacecraft and Rockets*, Vol. 43, No. 4, July–Aug. 2006, pp. 794–805. doi:10.2514/1.17413
- [10] Olds, A. D., Kluever, C. A., and Cupples, M. C., "Interplanetary Mission Design Using Differential Evolution," *Journal of Spacecraft and Rockets*, Vol. 44, No. 5, 2007, pp. 1060–1070. doi:10.2514/1.27242
- [11] Izzo, D., and Vinkó, T., "GTOPACT Trajectory Database," ESA [online database], <http://www.esa.int/gsp/ACT/inf/op/globopt.htm> [retrieved Sept. 2010].
- [12] Abdelkhalik, O., and Mortari, D., "N-Impulse Orbit Transfer Using Genetic Algorithms," *Journal of Spacecraft and Rockets*, Vol. 44, No. 2, March–April 2007, pp. 456–459. doi:10.2514/1.24701
- [13] Gad, A., Addanki, N., and Abdelkhalik, O., "N-Impulses Interplanetary Orbit Transfer Using Genetic Algorithm with Application to Mars Mission," 20th AAS/AIAA Space Flight Mechanics Meeting, American Astronautical Soc. Paper 10-167, Springfield, VA, Feb. 2010.
- [14] Kim, Y. H., and Spencer, D. B., "Optimal Spacecraft Rendezvous Using Genetic Algorithms," *Journal of Spacecraft and Rockets*, Vol. 39, No. 6, Nov. 2002, pp. 859–865. doi:10.2514/2.3908
- [15] Kim, R., Jung, O., and Bang, H., "A Computational Approach to Reduce the Revisit Time Using a Genetic Algorithm," *International Conference on Control, Automation and Systems*, Seoul, ROK, IEEE Publ., Piscataway, NJ, Oct. 2007, pp. 184–189. doi:10.1109/ICCAS.2007.4406905
- [16] Abdelkhalik, O., and Mortari, D., "Orbit Design for Ground Surveillance Using Genetic Algorithms," *Journal of Guidance*,

- Control, and Dynamics*, Vol. 29, No. 5, Sept.–Oct. 2006, pp. 1231–1235.
doi:10.2514/1.16722
- [17] Ely, T. A., Crossley, W. A., and Williams, E. A., “Satellite Constellation Design for Zonal Coverage Using Genetic Algorithms,” *Journal of the Astronautical Sciences*, Vol. 47, No. 3 and 4, July–Dec. 1999, pp. 207–228.
- [18] Rauwolf, G., and Coverstone-Carroll, V., “Near-Optimal Low-Thrust Orbit Transfer Generated by a Genetic Algorithms,” *Journal of Spacecraft and Rockets*, Vol. 33, No. 6, Nov.–Dec. 1996, pp. 859–862.
doi:10.2514/3.26850
- [19] Goldberg, D., *Genetic Algorithms in Search, Optimization, and Machine Learning*, Addison Wesley Longman, Boston, MA, 1989, pp. 59–88.
- [20] Dasgupta, D., and McGregor, D. R., “SGA : A Structured Genetic Algorithm,” *Parallel Problem Solving from Nature*, Elsevier, Brussels, Sept. 1992, pp. 145–154.
- [21] Kim, I. Y., and de Weck, O. L., “Variable Chromosome Length Genetic Algorithm for Progressive Refinement in Topology Optimization,” *Structural and Multidisciplinary Optimization*, Vol. 29, No. 6, 2005, pp. 445–456.
doi:10.1007/s00158-004-0498-5
- [22] Zhu, K., Li, J., and Baoyin, H., “Trajectory Optimization of the Exploration of Asteroids Using Swarm Intelligent Algorithms,” *Tsinghua Science and Technology*, Vol. 14, No. 2, 2009, pp. 7–11.
doi:10.1016/S1007-0214(10)70022-5
- [23] Gantovnik, V. B., Gurdal, Z., Watson, L. T., and Anderson-Cook, C. M., “Genetic Algorithm for Mixed Integer Nonlinear Programming Problems Using Separate Constraint Approximations,” *AIAA Journal*, Vol. 43, No. 8, 2005, pp. 1844–1849.
doi:10.2514/1.4191
- [24] Abdelkhalik, O., and Gad, A., “Optimization of Space Orbits Design for Earth Orbiting Missions,” *Acta Astronautica*, Vol. 68, Nos. 7–8, 2011, pp. 1307–1317.
doi: 10.1016/j.actaastro.2010.09.029
- [25] Vallado, D. A., and McClain, W. D., *Fundamentals of Astrodynamics and Applications*, 2nd ed., Microcosm Press and Kluwer Academic, New York, 2004, pp. 53–54.
- [26] Curtis, H., *Orbital Mechanics for Engineering Students*, Elsevier Butterworth-Heinemann, Burlington, MA, 2005, pp. 375–386.
- [27] Zimmerman, D. C., “GENETIC MATLAB Toolbox,” Software Package, Ver. 2.1, Univ. of Houston, TX, 1998.
- [28] Beasley, D., Bull, D. R., and Martin, R. R., “A Sequential Niche Technique for Multimodal Function Optimization,” *Evolutionary Computation*, Vol. 1, No. 2, 1993, pp. 101–125.
doi:10.1162/evco.1993.1.2.101

C. Kluever
Associate Editor